NeuroImage: Clinical 26 (2020) 102201

Contents lists available at ScienceDirect

NeuroImage: Clinical

journal homepage: www.elsevier.com/locate/ynicl

Voxel-based analysis of gray matter relaxation rates shows different correlation patterns for cognitive impairment and physical disability in relapsing-remitting multiple sclerosis

Maria Teresa Cassiano[a], Roberta Lanzillo[b], Bruno Alfano[c], Teresa Costabile[b], Marco Comerci[c], Anna Prinster[c], Marcello Moccia[b], Rosario Megna[c], Vincenzo Brescia Morra[b], Mario Quarantelli[c,1,*], Arturo Brunetti[a,1]

[a] Department of Advanced Biomedical Sciences, University "Federico II", Via Pansini, 5, 80131 Naples, Italy
[b] Department of Neurosciences, Reproductive Science and Odontostomatology, University "Federico II", Naples, Italy
[c] Biostructure and Bioimaging Institute, National Research Council, Via De Amicis, 95, 80145 Naples, Italy

ARTICLE INFO

Keywords:
Atrophy
Multiple sclerosis
Quantitative MRI
Relapsing/remitting
Cognitive impairment
Relaxation rates

ABSTRACT

Background: Regional analyses of markers of microstructural gray matter (GM) changes, including relaxation rates, have shown inconsistent correlations with physical and cognitive impairment in MS.
Objective: To assess voxelwise the correlation of the R1 and R2 relaxation rates with the physical and cognitive impairment in MS.
Methods: GM R1 and R2 relaxation rate maps were obtained in 241 relapsing-remitting MS patients by relaxometric segmentation of MRI studies. Correlations with the Expanded Disability Status Scale (EDSS) and the percentage of impaired cognitive test (Brief Repeatable Battery and Stroop Test, available in 186 patients) were assessed voxelwise, including voxel GM content as nuisance covariate to remove the effect of atrophy on the correlations.
Results: Extensive clusters of inverse correlation between EDSS and R2 were detected throughout the brain, while inverse correlations with R1 were mostly limited to perirolandic and supramarginal cortices. Cognitive impairment correlated negatively with R1, and to a lesser extent with R2, in the middle frontal, mesial temporal, midcingulate and medial parieto-occipital cortices.
Conclusion: In relapsing-remitting MS patients, GM microstructural changes correlate diffusely with physical disability, independent of atrophy, with a preferential role of the sensorimotor cortices. Neuronal damage in the limbic system and dorsolateral prefrontal cortices correlates with cognitive dysfunction.

1. Introduction

Gray matter (GM) damage in Multiple Sclerosis (MS), related to both cortical lesion accrual and normal-appearing gray matter microstructural changes (Filippi et al., 2012), occurs largely independent of white matter (WM) lesions (Bodini et al., 2016; Kutzelnigg et al., 2005), and shows a significant correlation with clinical disability (Filippi et al., 2012). GM involvement in MS has been extensively studied using MRI, which allows to study both macro- (e.g., GM atrophy) and microstructural (e.g., changes in water diffusion, macromolecule interactions and relaxometric properties) GM alterations.

In particular, studies of regional atrophy have shown that GM loss in relapsing-remitting multiple sclerosis (RR-MS) preferentially affects the deep gray matter, pre/postcentral regions and the cingulate, GM volume loss in left rolandic cortex significantly correlating with motor disability (Lansley et al., 2013). In addition, evidence points towards the preferential atrophy of specific brain structures in cognitively impaired patients (Kolbe et al., 2014; Popescu et al., 2016; Preziosa et al., 2016; Riccitelli et al., 2011), with several neuropsychological test scores correlating with relevant structures (Achiron et al., 2013; Bergsland et al., 2016; Bisecco et al., 2018; Ernst et al., 2015; Geisseler et al., 2016; Nocentini et al., 2014; Sbardella et al., 2013; van de Pavert et al., 2016; Zhang et al., 2016).

In addition to regional atrophy, also GM microstructural alterations,

* Corresponding author.
E-mail address: quarante@unina.it (M. Quarantelli).
[1] MQ and AB share senior authorship

https://doi.org/10.1016/j.nicl.2020.102201
Received 17 September 2019; Received in revised form 13 January 2020; Accepted 28 January 2020
Available online 30 January 2020

as assessed using Diffusion tensor Imaging (DTI) (Llufriu et al., 2014), Magnetization Transfer Ratio (MTR) (Khaleeli et al., 2007; Ranjeva et al., 2005), and R2* relaxation rate (Louapre et al., 2016b,a; Wen et al., 2015), have shown preferential correlations with cognitive scores in cortical regions relevant to the tested cognitive domains. However, it is not clear whether and to what extent these correlations are independent from macroscopic tissue damage (i.e., whether they are driven by GM atrophy).

Unlike cognitive measures, physical disability scores show a less straightforward pattern of correlations with microstructural GM damage, since voxel-based analyses have so far provided conflicting results, while global GM microstructural integrity measures correlate in general well with physical disability.

In particular, most studies have shown correlation of GM MTR parameters, averaged over the whole GM, with physical disability in RR-MS (Davies et al., 2004a; Ge et al., 2001), Clinically Isolated Syndromes suggestive of MS (Crespy et al., 2011), Secondary (Hayton et al., 2009) and Primary Progressive (Dehmeshki et al., 2003; Ramio-Torrenta et al., 2006; Rovaris et al., 2008) MS patients, as well as in mixed patient groups (Davies et al., 2004b; Samson et al., 2014, 2013; Vrenken et al., 2007; Yarnykh et al., 2015).

Correlation with physical disability appeared even more significant when GM MTR was combined with R1 in the calculation of macromolecular proton fraction (Yarnykh et al., 2015), in line with the known correlation between GM relaxation rates and the Expanded Disability Status Scale (EDSS) (Gracien et al., 2016; Megna et al., 2019).

Similarly, global GM DTI-derived measures have been shown to correlate with EDSS in RR, although not in the early stages (Griffin et al., 2001; Yu et al., 2008) and in the progressive forms (Ammitzbøll et al., 2018) of the disease.

Despite strong evidences for correlations between the overall GM microstructural integrity and physical disability, the available voxel-based analyses, limited to R2* (Wen et al., 2015) and diffusivity (Senda et al., 2012) maps, have failed so far in localizing these correlations in the cortex, while ROI-based analyses of R2* of the deep GM structures have shown such a correlation in most (Baranovicova et al., 2017; Quinn et al., 2014; Rudko et al., 2014; Wen et al., 2015) but not all (Khalil et al., 2015) cases.

Aim of this retrospective study was to assess the role of regional microstructural GM changes, as measured by a voxel-based analysis of R1 and R2 relaxation rate maps, in determining physical disability and cognitive impairment in RR-MS, taking also into account the effect of atrophy by covarying at voxel level for the GM concentration.

2. Material and methods

2.1. Patients

MRI studies from 241 patients with clinically definite RR-MS according to the McDonald criteria (McDonald et al., 2001) (141 females; mean age 34.6 ± 7.9 y; disease duration 4,9 ± 5.4 y; EDSS 2.4 ± 0.9, range 1–5) were retrospectively analyzed. Patients were selected from the patient population of the MS Center of the University "Federico II" of Naples (Italy) based on the availability of an MRI study suitable for multiparametric relaxometric segmentation, along with an EDSS collected within 1 month from the MRI.

Patients < 18 year, or with other clinically significant neurological, cerebrovascular or psychiatric disease were excluded, as well as those who had been treated at any time before the MRI with monoclonal antibodies, cytotoxic or immunosuppressive therapies (steroids were deemed acceptable unless administered in the month preceding the MRI scan).

Results of the analysis of the mean R1 and R2 values of GM, WM and WM lesions from these patients have been published separately in a previous work (Megna et al., 2019).

All studies have been approved by the Institutional Review Board of the "Federico II" University, and all participants gave informed written consent.

2.2. Clinical and neuropsychological assessment

The results of a battery of cognitive tests, including Rao's Brief Repeatable Battery (BRB) (Rao, 1991) and the Stroop test (Barbarotto et al., 1998), acquired within one month from the MRI scan, were available in 186 patients.

Briefly, the BRB tests probe verbal learning and long term memory (by the Selective Reminding Test), visuospatial learning (10/36 Spatial Recall Test), information processing speed (Symbol Digit Modalities Test), sustained attention (Paced Auditory Serial Addition Test), and semantic fluency (Word List Generation).

In addition, the ability to inhibit automatic responses was probed by the Stroop test.

For the present work, a Cognitive Index (CI) was calculated as the percentage of impaired cognitive tests (Megna et al., 2019), compared to available normative data (Amato et al., 2006; Barbarotto et al., 1998).

2.3. MRI

All MRI studies, collected as part of patient participation in clinical trials, observational studies or clinical practice, were acquired on the same 1.5T scanner (Intera, Philips Medical Systems, the Netherlands).

Acquisition protocols (including a single-echo T1-weighted and a double-echo PD/T2-weighted sequence with equal echo time for T1 and PD volumes, as required by the relaxation rate calculation procedure) are reported in Table 1. Over time, 3 similar acquisition protocols, differing for slice thickness, Repetition and Echo time have been used, with one protocol (Protocol C in Table 1) being also split in two separated protocols, as two different water-fat shifts had been used over time. Additional details on MRI sequences can be found elsewhere (Megna et al., 2019).

For each study, pre-processing steps (summarized in Fig. 1) included the following:

- Automated rigid body co-registration (Ashburner and Friston, 1997) of the T1w and PD/T2w volumes using the Statistical Parametric Mapping software (SPM, https://www.fil.ion.ucl.ac.uk/spm), using normalized mutual information with SPM8 default parameters, to take care of possible between-sequence head movements.
- Calculation of the R1, R2 and PD maps, performed according to the general formula of the signal intensity in the transverse steady state for conventional spin-echo images (Bakker et al., 1984), as described in detail elsewhere (Alfano et al., 1997, 1995, 1992).
- Segmentation of the co-registered MRI volumes into GM, normal and abnormal WM, and cerebro-spinal fluid, using a fully automated relaxometric method (Alfano et al., 2000; Prinster et al., 2010). Shortly, after a preliminary segmentation performed by assigning the voxels with relaxation rates "typical" for a specific tissue to the

Table 1
MRI sequences used for multiparametric relaxometric segmentation. DP/T2 sequences in protocol C were acquired with a water/fat shift of either 0.7 (95 patients) or 1.2 (53 patients) pixels. Accordingly, in the analysis four separate acquisition protocols were included as nuisance covariate.

Protocol	n	TR/TE (ms)		Voxel size (mm^3)
		T1-weighted (2 averages)	PD-/T2-weighted	
A (32 slices)	60	600/15	2200/15–90	0.94•0.94•4
B (32 slices)	86	520/15	1800/15–90	0.86•0.86•4
C (48 slices)	148	500/10	2300/10–80	0.98•0.98•3

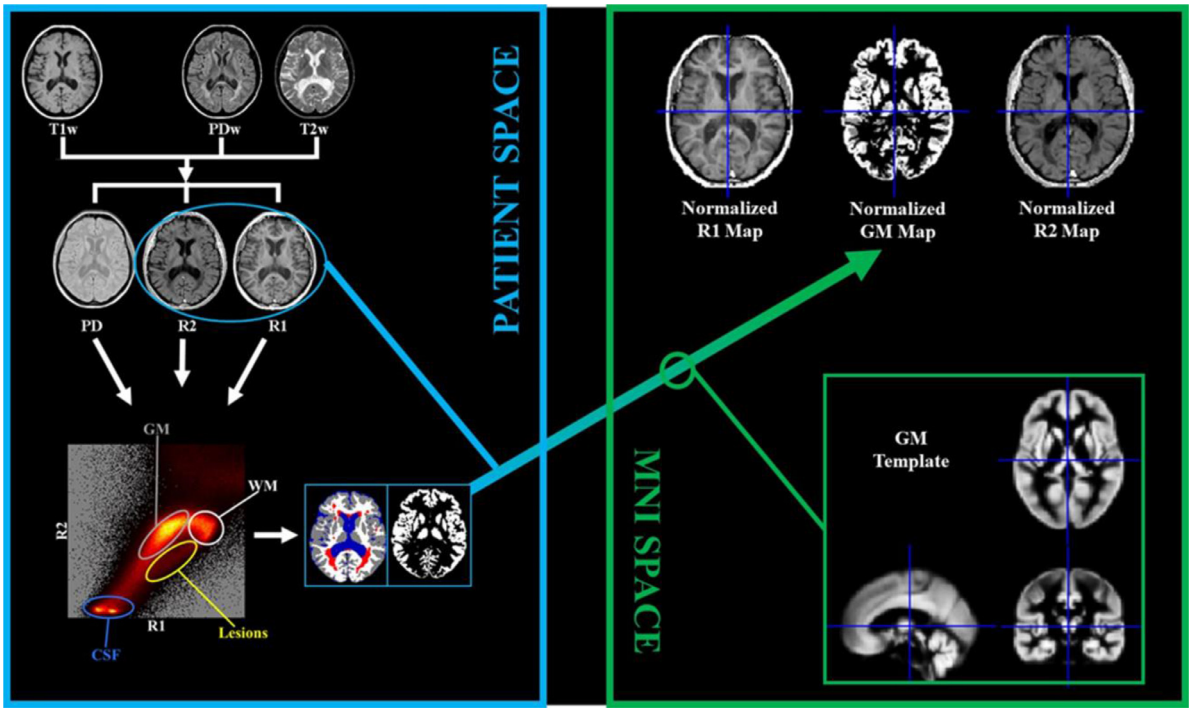

Fig. 1. Diagram of the pre-processing procedure. From the T1- DP- and T2-weighted images (upper row in the left box), the R1, R2 and PD volumes are calculated. Brain voxels are then segmented based on the corresponding R1, R2 and PD values (lower row in left box). The resulting GM map is spatially normalized to the GM template provided by SPM (lower part of the right box), and resulting spatial normalization parameters are also applied to R1 and R2 volumes (inherently registered to the segmented GM), providing the spatially normalized maps which are entered, after smoothing, in the voxel-based statistical analysis.

corresponding tissue maps, the remaining voxels are assigned to a specific tissue based on a combined probability approach, which takes into account also the relaxation rates of the surrounding voxels.

- Notably, this method, which has shown an inter-study standard deviation of 1.1% in repeated normal tissue fractional volumes measurements (Alfano et al., 1998), and an excellent correlation with the manual definition of the MS lesions ($R = 0.993$ at linear regression analysis, 87.3% sensitivity (Alfano et al., 2000)), is not affected by lesion-associated bias in the measure of brain tissue volumes in MS (Prinster et al., 2006), so that it does not require lesion masking or filling prior to segmentation.
- Spatial normalization (Ashburner and Friston, 1999) of the GM maps to the stereotactic space of the Montreal Neurological Institute (MNI) space using the GM template provided by SPM8.
- Application of the resulting spatial normalization matrix to the R1 and R2 maps.
- Smoothing (8 mm, full-width at half maximum) of the spatially normalized GM, R1 and R2 maps, to reduce confounding by individual residual anatomical variations and to render the data normally distributed, as required by the Gaussian random field models used for adjusting *p*-values for familywise error (Friston et al., 1995).

2.4. Statistical analysis

Correlation of R1 and R2 with EDSS and CI were separately assessed voxelwise using the "Biological Parameter Mapping" software package (Casanova et al., 2007), including as nuisance covariates age, sex, MRI protocol, disease duration, and T2-lesion volume, along with the voxelwise GM content provided by each patient's smoothed, spatially normalized GM map.

Covarying at voxel level by the GM map allowed assessing the correlations between relaxation rates and clinical scores independent of the local degree of GM atrophy.

As the focus of the work was the correlation between GM relaxation rates and clinical scores, the analysis was restricted by a study-specific GM mask, defined by thresholding at 40% (as defined by visually assessing the anatomic meaningfulness of the resulting mask) the mean of the unsmoothed, spatially normalized GM maps.

Where significant correlations with CI emerged, the analysis was replicated including also the EDSS as additional nuisance covariate, to assess whether these were independent of physical disability.

In addition, to allow for comparison with other studies not focusing specifically on GM and/or not including GM volume correction, these same analyses were replicated using a brain parenchyma mask, obtained thresholding at 40% the average of the unsmoothed normalized brain tissue maps (obtained as the sum of GM, normal-appearing WM and WM lesion masks). Results of these ancillary analyses are reported in the Supplementary data.

For all voxelwise analyses, significance was set to $p < 0.05$, corrected for family-wise error (FWE) at cluster level, following a cluster-defining threshold of 0.001.

3. Results

Clusters of significant correlation with EDSS and CI are shown in Fig. 2 for R1 and in Fig. 3 for R2, superimposed on the average of the spatially normalized GM maps of the 241 patients.

Cluster dimensions are reported in Table 2 for R1 and Table 3 for R2, respectively, along with local maxima coordinates and corresponding anatomical labels (Tzourio-Mazoyer et al., 2002).

When testing correlations between CI and GM relaxation rates, limited clusters of significant inverse correlation with R2 were found bilaterally in the left middle frontal and precentral gyri, and in the parahippocampal GM on the right. Larger clusters of inverse correlation with R1 were found bilaterally in the middle frontal gyri and mesial temporal GM, as well as in the left midcingulate and in the right medial parieto-occipital cortices.

When EDSS was included in the model, no cluster of correlation

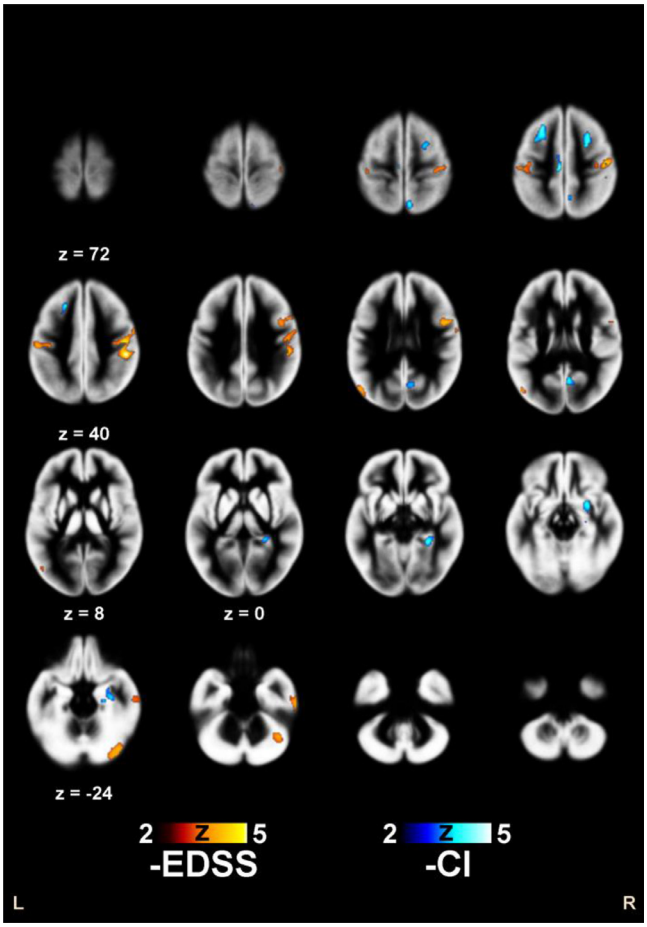

Fig. 2. Clusters of significant inverse correlation of R1 with EDSS and CI, superimposed on the average of the spatially normalized GM maps of the 241 patients. Z coordinates are in mm in the MNI space.

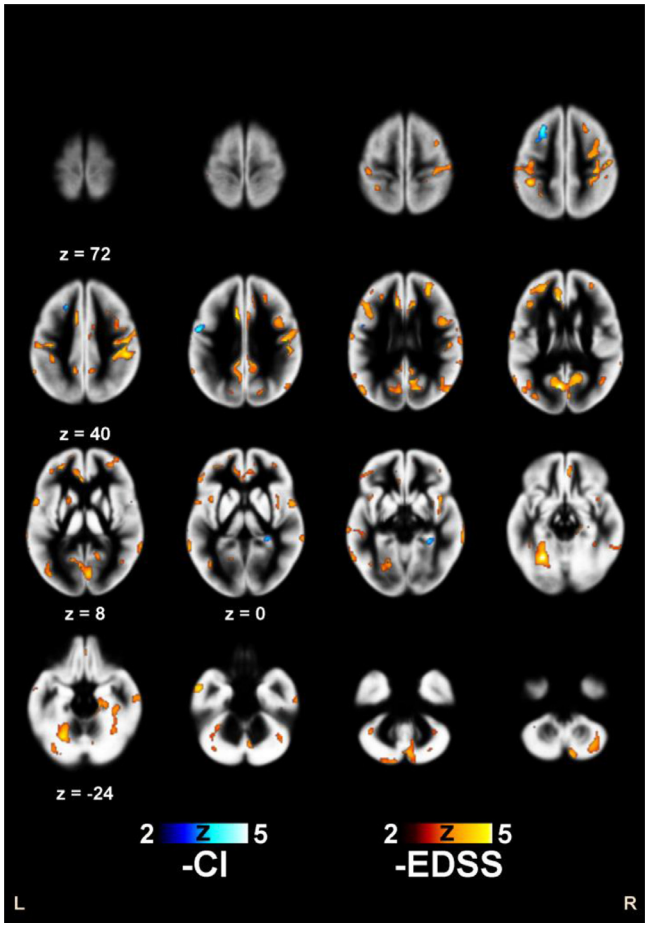

Fig. 3. Clusters of significant inverse correlation of R2 with EDSS and CI, superimposed on the average of the spatially normalized GM maps of the 241 patients. Z coordinates are in mm in the MNI space.

between CI and R2 remained significant, while significant clusters of inverse correlation could still be demonstrated for R1 in the precuneus, in dorso-lateral prefrontal regions, and in the midcingulate cortex.

When testing correlations between EDSS and GM relaxation rates, extensive clusters of inverse correlation with R2 values were present bilaterally throughout the brain, the most significant being in the right pre- and post-central gyri. For R1, clusters of inverse correlation with EDSS were less diffuse, restricted to bilateral perirolandic and supramarginal cortices, with additional clusters in the Crus I of the right cerebellar hemisphere, and in the posterior part of the left middle temporal gyrus.

The same analysis, when performed using the brain parenchyma mask, confirmed these results for GM, while showing additional clusters of inverse correlation of R1 with the cognitive index in the posterior part of the corpus callosum, and in the iuxtacortical WM of the right posterior insula and temporo-occipital cortex on the right (Supplementary Fig. 1). Similarly, R2 showed additional clusters of inverse correlation with EDSS in the ventral ponto-mesencephalic regions, and with CI in the posterior corpus callosum and iuxtacortical occipital WM on the left (Supplementary Fig. 2).

Results did not change significantly when the same analyses carried out without covarying at voxel level by the GM map (Supplementary Figs. 3 and 4).

4. Discussion

Current results show, in a large sample of RR-MS, that GM relaxation rates have distinct patterns of correlation with physical disability and cognitive impairment across the cortex, independent of atrophy.

In particular, R2 confirmed a significant inverse correlation with motor function, as probed by EDSS, throughout the cerebral and cerebellar cortices, with perirolandic regions showing the strongest correlation. The relevance of motor cortex involvement for EDSS was confirmed when analyzing R1 maps, which showed a clearly preferential correlation in the rolandic cortices.

On the other hand, CI correlated negatively with R1 in the dorsolateral prefrontal cortices, mid-cingulate, precuneus, and in the right medial temporal GM, and showed a similar pattern of correlation (although more limited in extension) with R2.

It is presently unclear whether these different patterns are also subtended by different pathological phenomena. Although correlation between R1 and R2 throughout brain tissues is overall quite strong, these two relaxation rates are only partly influenced by the same biological phenomena. In GM in particular, while R1 and R2 are both lowered in cortical lesions, they seem to be differentially affected by pathological changes, with R2 being influenced mainly by demyelination, and R1 by neuronal loss (Schmierer et al., 2010; Seewann et al., 2011), and indeed they behave differently in demyelinated cortex, where their ratio is significantly affected (Nakamura et al., 2017).

While the definition of the different pathological bases of these two rates was beyond the scope of the present work, we think that their different behaviors in our results (in particular, the more extensive correlations of EDSS with R2 compared to R1, and the opposite pattern when testing their correlations with CI), hint at different pathological substrates.

It is thus tempting to infer that cognitive impairment is related to

Table 2
Clusters of significant ($p < 0.05$, FWE-corrected at cluster level) correlation of R1 with Cognitive Index and EDSS, including in the model age, sex, DD and LL as nuisance covariates, along with GM map as voxelwise nuisance covariate. Results of the analysis without and with EDSS included as nuisance covariate are reported.

	Cluster#			MNI (mm)			
		cc	T	X	Y	Z	Structure
EDSS vs. R1 ($n = 241$)	1	6.2	5.28	50	−30	38	R SupraMarginal Gyrus
			4.66	50	−16	40	R Postcentral Gyrus
			3.62	36	−18	44	R Precentral Gyrus
	2	2.5	4.26	42	−70	−26	R Cerebellum (Crus 1)
	3	1.8	4.26	−54	−20	42	L SupraMarginal Gyrus
			3.81	−40	−20	42	L Postcentral Gyrus
	4	1.7	4.3	48	8	26	R IFG (p. Opercularis)
			3.68	54	12	32	R Precentral Gyrus
	5	1.1	4.06	−50	−72	22	L Middle Temporal Gyrus
CI vs. R1 ($n = 186$)	1	2.0	4.38	−24	26	46	L Middle Frontal Gyrus
	2	1.8	4.02	28	4	−16	R Amygdala
			3.75	32	−10	−24	R Hippocampus
			3.61	24	−14	−24	R ParaHippocampal Gyrus
	3	1.4	4.18	28	14	46	R Middle Frontal Gyrus
	4	1.3	4.06	6	−62	16	R Calcarine Gyrus
			3.71	8	−68	26	R Cuneus
	5	1.1	4.21	28	−38	−6	R ParaHippocampal Gyrus
			3.26	36	−28	−10	R Hippocampus
	6	0.8	4.38	−6	−22	48	L Middle cingulate & paracingulate gyri
	7	0.8	4.07	8	−66	58	R Precuneus
CI vs. R1 controlled for EDSS ($n = 186$)	1	1.6	4.59	6	−64	54	R Precuneus
			3.73	−6	−66	62	L Precuneus
	2	1.5	4.12	−22	26	44	L Middle Frontal Gyrus
	3	1.2	4.65	−4	20	46	L Posterior-Medial Frontal
	4	1.0	4.41	−6	−22	48	L Middle cingulate & paracingulate gyri
	5	0.8	3.86	28	14	48	R Middle Frontal Gyrus
			3.39	24	2	54	R Superior Frontal Gyrus

Table 3
Clusters of significant ($p < 0.05$, FWE-corrected at cluster level) inverse correlation of R2 with Cognitive Index and EDSS, including in the model age, sex, DD and LL. No clusters of significant correlation between R2 and CI were present when EDSS was included in the model.

	Cluste #			MNI (mm)			Structure
		cc	T	X	Y	Z	
EDSS vs. R2 ($n = 241$)	1	14.4	4.94	48	−16	38	R Postcentral Gyrus
			4.41	36	−16	44	R Precentral Gyrus
			4.16	38	6	52	R Middle Frontal Gyrus
			3.81	52	−20	24	R SupraMarginal Gyrus
	2	12.0	5.25	−26	−58	−18	L Cerebellum (VI)
			4.48	−26	−68	−12	L Fusiform Gyrus
			4.39	−50	−72	22	L Middle Temporal Gyrus
			4.14	−36	−72	−28	L Cerebellum (Crus 1)
			4.04	−26	−46	−16	L Fusiform Gyrus
			3.77	−40	−64	−2	L Middle Occipital Gyrus
	3	8.4	5.33	−6	−70	18	L Calcarine Gyrus
			4.98	10	−60	22	R Precuneus
			4.48	6	−78	10	R Calcarine Gyrus
			4.35	14	−70	22	R Cuneus
			3.68	−14	−62	2	L Linual Gyrus
			3.58	−18	−72	26	L Superior Occipital Gyrus
			3.47	−10	−78	26	L Cuneus
	4	4.8	5.27	−8	34	16	L Anterior cingulate & paracingulate gyri
			4.81	−8	12	32	L Middle cingulate & paracingulate gyri
			3.77	6	44	2	R Anterior cingulate & paracingulate gyri
			3.45	12	54	2	R Superior Medial Gyrus
	5	3.6	4.2	−40	−20	42	L Postcentral Gyrus
			4.12	−54	−22	44	L Inferior Parietal Lobule
	6	2.7	4.71	28	44	26	R Middle Frontal Gyrus
			3.45	42	46	−6	R IFG (p. Orbitalis)
	7	2.6	4.69	−26	48	12	L Middle Frontal Gyrus
			4.2	−16	62	4	L Superior Frontal Gyrus
			3.24	−16	60	−4	L Superior Orbital Gyrus
	8	2.5	4.43	8	−78	−44	R Cerebellum (VII)
			4.16	8	−68	−34	R Cerebellum (VIII)
CI vs. R2 ($n = 186$)	1	1.6	4.49	−24	26	46	L Middle Frontal Gyrus
	2	0.7	4.27	−50	4	28	L Precentral Gyrus
	3	0.7	3.8	28	−38	−6	R ParaHippocampal Gyrus

major changes occurring in specific cortical structures (e.g., neuronal loss), while motor deficits are the consequence of a non-specific damage in the motor cortices (e.g., demyelination, reactive gliosis, and/or inflammatory edema). However, further studies are needed to allow to draw firm conclusions on pathology correlates of these MRI measures.

The present results add to the current limited and apparently conflicting data on regional correlations between microstructural GM alterations and physical disability. In particular, R2 (Lund et al., 2012), R2* (Wen et al., 2015) and DTI studies (Senda et al., 2012) did not find similar correlations at 3 Tesla, while extensive correlations between R2* and EDSS, independent of atrophy, have been shown throughout the cortex at 7T (Mainero et al., 2015).

The latter findings are indeed in line with current results, which show an extensive pattern of correlation with EDSS, independent of atrophy, particularly significant in the rolandic cortices. Additional studies on further independent datasets are thus needed to confirm this pattern, and to clarify the strength and clinical significance of these correlations.

Previous ROI-based analyses of R2* of the deep GM structures have shown a correlation with physical disability in most (Baranovicova et al., 2017; Quinn et al., 2014; Rudko et al., 2014), but not all cases (Khalil et al., 2015; Wen et al., 2015).

It is however not surprising that in our study a significant correlations in deep GM did not emerge, given the relative lack of sensitivity of R2 measures to iron accumulation, which is thought to be behind the increases of R2* that showed correlation with EDSS in some of these studies.

The pattern of correlations with CI partly conflicts with those from previous studies that have probed the correlations between microstructural GM integrity and cognitive status in MS. In particular, Llufriu et al. (2014) have assessed the correlation of diffusivity parameters with the BRB subtests in RR-MS, showing a correlation of radial diffusivity (a putative measure of myelination) with the Selective Reminding Test in several GM regions. These included the occipital (i.e. angular, calcarine, lingual and fusiform cortex) medial and lateral temporal and thalamic GM, as well as in precuneus and fronto-orbital cortex, and with the Symbol Digit Modalities Test in the left occipital cortex, cerebellum and anterior insula. Reasons for this partial discrepancy may be due to differences in tissue properties probed by relaxation rates and DTI, and to the different analysis strategy, which in that case did not include correction for atrophy. This critical difference, coupled to the larger dataset used for the present study, may explain the different patterns of correlation.

Similarly, in Clinically Isolated Syndromes suggestive of MS, sustained attention scores have been shown to correlate with MTR in right motor cortex and left supramarginal cortex (Ranjeva et al., 2006), although again this was obtained in a small number of subjects, without correcting for GM atrophy.

Also, a preliminary study of regional correlates of cognitive and physical disability in RR-MS, carried out by voxel-wise analysis of T2 maps (Lund et al., 2012) has shown the correlation to be essentially limited to WM and subcortical structures, without significant cortical involvement, for cognitive test scores. While differences in the methods of cognitive assessment may here explain differences in results for CI, the lack of correlations in that case may be partly due to the limited number of subjects, coupled with a significant heterogeneity of scanner/protocol combinations (50 subjects studied using 6 different scanner/protocol combinations).

On the other hand, consistent with our results, other studies have shown direct correlation, independent of atrophy, of R2* with cognitive status in MS patients with mixed disease courses, in cortical regions including parahippocampus, precuneus and prefrontal GM (Louapre et al., 2016b; Wen et al., 2015).

Along this line, correlations with CI of GM relaxation rates in precuneus, medial frontal and medial temporal cortices seem to point to the involvement of the main hubs of the limbic circuits, known to play a role in cognitive impairment of MS patients, as shown by ROI analyses of volumetric, relaxometric and DTI data (Keser et al., 2018, 2017; Wen et al., 2017).

Some limitations of our work should be considered when interpreting the present results:

The use of conventional spin-echo images for calculating the relaxation rate maps, while allowing to collect retrospectively a large data set, have imposed a limited axial resolution, resulting in substantial partial volume effects. Studies using recently introduced isotropic 3 D-sequences suitable for relaxometric analysis (Deoni et al., 2008; Marques et al., 2010; Palma et al., 2015), are thus needed to confirm these results.

As this was a retrospective study, data from healthy controls were not available, so that no inferences can be done on the normality of the relaxation rates in these patients. However, several previous studies have shown alterations of GM relaxation rates in MS (Neema et al., 2007), including a recent one in which the same relaxometric segmentation method as in the present work was used (Pota et al., 2019). In that work R1 and R2 relaxation rates averaged over the whole GM, estimated as per MRI protocol A of the present work, were assessed in a group of RR-MS patients and a small group of healthy controls. Results showed that the mean GM R2 differences between the two groups were highly significant, while R1 differences did not reach significance, in line with the overall more limited correlations showed by R1 with the clinical scores in our data. Further studies are thus needed to clarify the spatial relationship between the present results and the alterations of GM relaxation rates previously documented in MS.

In the present study. R2 maps have been calculated by mono-exponential fitting of data from two echo times, close respectively to the T2 of myelin (~20 ms) and free water (~80 ms) (Laule et al., 2006). Accordingly, the resulting R2 values can be affected by changes in tissue composition in terms of the relative prevalence of these two water components, and/or by alterations of their relaxation rates. Studies using multi-echo sequences allowing multiexponential fitting, and correlation with other measures of myelin integrity (e.g. by DTI), are expected to allow to separate the contributions from these two compartments.

For the present study, GM voxels were identified by a relaxometric segmentation method (in which the probability of voxels to be classified as GM depends chiefly on its relaxation rates, which must be typical of that tissue). This introduces a possible bias, as where severe relaxation rate changes are introduced by pathology, missegmentation of GM can occur, thus reducing our capacity to detect possible correlations with clinical scores through two mechanisms:

1) apparent local atrophy due to GM missegmentation results in overcorrection when covarying for local GM volume, as was done here using the biological parametric mapping approach;
2) the possible presence of regions where GM pathology (and thus relaxation rate changes) is consistently more pronounced, which may result in a locally more restrictive study-specific GM mask, thus excluding those voxels from the analysis.

However, in the ancillary analyses GM results were confirmed when using a brain parenchyma mask, which included also normal-appearing and abnormal WM, and both with and without correction for GM volume.

Accordingly, we think that the main findings of the work are not significantly affected by this mechanism. Further studies, using independent segmentation and relaxation rate calculation methods, are however warranted to fully rule out this potential confounding factor.

5. Conclusion

We have shown in a large group of RR-MS patients significant regional correlations between R1 and R2 relaxation rates and both

cognitive and physical impairment, independent of disease duration, T2-lesion load, and GM atrophy.

The results suggest an extensive correlation in the cortex between microstructural changes and physical disability, with a preferential role of the sensorimotor cortices, where neuronal loss may play a specific role. On the other hand, neuronal loss in the limbic system and dorsolateral prefrontal cortices appear more strictly related to the cognitive symptoms.

Further studies are needed, possibly coupling other measures of microstructural integrity (e.g. MTR and DTI-derived) to relaxation rates, to confirm these findings and to clarify the pathophysiological meaning of these correlations.

Disclosure

R.L. received personal fees for public speaking or consultancy from Merck, Novartis, Biogen, Genzyme, Teva and Almirall.

M.M. declares that he has received honoraria and support for travelling from Almirall, Coloplast, Genzyme and Merck Serono.

V.B.M. received personal fees for public speaking or consultancy from Bayer, Mylan, Merck, Novartis, Biogen, Genzyme, Teva and Almirall.

CRediT authorship contribution statement

Maria Teresa Cassiano: Visualization, Formal analysis, Writing - original draft. **Roberta Lanzillo:** Investigation. **Bruno Alfano:** Methodology, Funding acquisition. **Teresa Costabile:** Investigation. **Marco Comerci:** Formal analysis, Software, Data curation. **Anna Prinster:** Formal analysis, Software, Data curation. **Marcello Moccia:** Investigation. **Rosario Megna:** Formal analysis, Software, Data curation. **Vincenzo Brescia Morra:** Conceptualization, Methodology, Investigation. **Mario Quarantelli:** Conceptualization, Investigation, Project administration, Funding acquisition, Writing - review & editing. **Arturo Brunetti:** Conceptualization, Methodology, Resources.

Declaration of Competing Interest

None.

Acknowledgments

Funding by the CNR Strategic Project “The Aging: Technological and Molecular Innovations Aiming to Improve the Health of Older Citizens” (http://www.progettoinvecchiamento.it) and by the Italian Ministry for Education, University and Research (Project MOLIM ONCOBRAIN LAB) is gratefully acknowledged.

Supplementary materials

Supplementary material associated with this article can be found, in the online version, at doi:10.1016/j.nicl.2020.102201.

References

Achiron, A., Chapman, J., Tal, S., Bercovich, E., Gil, H., Achiron, A., 2013. Superior temporal gyrus thickness correlates with cognitive performance in multiple sclerosis. Brain Struct. Funct. 218, 943–950. https://doi.org/10.1007/s00429-012-0440-3.

Alfano, B., Brunetti, A., Arpaia, M., Ciarmiello, A., Covelli, E.M., Salvatore, M., 1995. Multiparametric display of spin-echo data from MR studies of brain. J. Magn. Reson. Imaging 5, 217–225.

Alfano, B., Brunetti, A., Ciarmiello, A., Salvatore, M., 1992. Simultaneous display of multiple mr parameters with “quantitative magnetic color imaging. J. Comput. Assist. Tomogr. 16, 634–640. https://doi.org/10.1097/00004728-199207000-00025.

Alfano, B., Brunetti, A., Covelli, E.M., Quarantelli, M., Panico, M.R., Ciarmiello, A., Salvatore, M., 1997. Unsupervised, automated segmentation of the normal brain using a multispectral relaxometric magnetic resonance approach. Magn. Reson. Med. 37, 84–93. https://doi.org/10.1002/mrm.1910370113.

Alfano, B., Brunetti, A., Larobina, M., Quarantelli, M., Tedeschi, E., Ciarmiello, A., Covelli, E.M., Salvatore, M., 2000. Automated segmentation and measurement of global white matter lesion volume in patients with multiple sclerosis. J. Magn. Reson. Imaging 12, 799–807 10.1002/1522-2586(200012)12:6<799::AID-JMRI2>3.0.CO;2-# [pii].

Alfano, B., Quarantelli, M., Brunetti, A., Larobina, M., Covelli, E.M., Tedeschi, E., Salvatore, M., 1998. Reproducibility of intracranial volume measurement by unsupervised multispectral brain segmentation. Magn. Reson. Med. 39, 497–499. https://doi.org/10.1002/mrm.1910390321.

Amato, M.P., Portaccio, E., Goretti, B., Zipoli, V., Ricchiuti, L., De Caro, M.F., Patti, F., Vecchio, R., Sorbi, S., Trojano, M., 2006. The Rao’s Brief Repeatable Battery and Stroop Test: normative values with age, education and gender corrections in an Italian population. Mult. Scler. 12, 787–793. https://doi.org/10.1177/1352458506070933.

Ammitzbøll, C., Dyrby, T.B., Lyksborg, M., Schreiber, K., Ratzer, R., Romme Christensen, J., Iversen, P., Magyari, M., Garde, E., Sørensen, P.S., Siebner, H.R., Sellebjerg, F., 2018. Disability in progressive MS is associated with T2 lesion changes. Mult. Scler. Relat. Disord. 20, 73–77. https://doi.org/10.1016/j.msard.2017.12.010.

Ashburner, J., Friston, K., 1997. Multimodal image coregistration and partitioning – a unified framework. Neuroimage 6, 209–217. https://doi.org/10.1006/nimg.1997.0290.

Ashburner, J., Friston, K.J., 1999. Nonlinear spatial normalization using basis functions. Hum. Brain Mapp. 7, 254–266.

Bakker, C.J., de Graaf, C.N., van Dijk, P., 1984. Derivation of quantitative information in NMR imaging: a phantom study. Phys. Med. Biol. 29, 1511–1525.

Baranovicova, E., Kantorova, E., Kalenska, D., Lichardusova, L., Bittsan-, M., Dobrota, D., 2017. Thalamic paramagnetic iron by T2* relaxometry correlates with severity of multiple sclerosis. J. Biomed. Res. 31, 301–305. https://doi.org/10.7555/jbr.31.20160023.

Barbarotto, R., Laiacona, M., Frosio, R., Vecchio, M., Farinato, A., Capitani, E., 1998. A normative study on visual reaction times and two Stroop colour-word tests. Ital. J. Neurol. Sci. 19, 161–170. https://doi.org/10.1007/BF00831566.

Bergsland, N., Zivadinov, R., Dwyer, M.G., Weinstock-Guttman, B., Benedict, R.H.B., 2016. Localized atrophy of the thalamus and slowed cognitive processing speed in MS patients. Mult. Scler. 22, 1327–1336. https://doi.org/10.1177/1352458515616204.

Bisecco, A., Stamenova, S., Caiazzo, G., d’Ambrosio, A., Sacco, R., Docimo, R., Esposito, S., Cirillo, M., Esposito, F., Bonavita, S., Tedeschi, G., Gallo, A., 2018. Attention and processing speed performance in multiple sclerosis is mostly related to thalamic volume. Brain Imaging Behav. 12, 20–28. https://doi.org/10.1007/s11682-016-9667-6.

Bodini, B., Chard, D., Altmann, D.R., Tozer, D., Miller, D.H., Thompson, A.J., Wheeler-Kingshott, C., Ciccarelli, O., 2016. White and gray matter damage in primary progressive MS: the chicken or the egg? Neurology. https://doi.org/10.1212/WNL.0000000000002237.

Casanova, R., Srikanth, R., Baer, A., Laurienti, P.J., Burdette, J.H., Hayasaka, S., Flowers, L., Wood, F., Maldjian, J.A., 2007. Biological parametric mapping: a statistical toolbox for multimodality brain image analysis. Neuroimage 34, 137–143. https://doi.org/10.1016/j.neuroimage.2006.09.011.

Crespy, L., Zaaraoui, W., Lemaire, M., Rico, A., Faivre, A., Reuter, F., Malikova, I., Confort-Gouny, S., Cozzone, P.J., Pelletier, J., Ranjeva, J.-P., Audoin, B., 2011. Prevalence of grey matter pathology in early multiple sclerosis assessed by magnetization transfer ratio imaging. PLoS One 6https://doi.org/10.1371/journal.pone.0024969. e24969.

Davies, G.R., Ramió-Torrentà, L., Hadjiprocopis, A., Chard, D.T., Griffin, C.M.B., Rashid, W., Barker, G.J., Kapoor, R., Thompson, A.J., Miller, D.H., 2004a. Evidence for grey matter MTR abnormality in minimally disabled patients with early relapsing-remitting multiple sclerosis. J. Neurol Neurosurg. Psychiatry 75, 998–1002. https://doi.org/10.1136/jnnp.2003.021915.

Davies, G.R., Tozer, D.J., Cercignani, M., Ramani, A., Dalton, C.M., Thompson, A.J., Barker, G.J., Tofts, P.S., Miller, D.H., 2004b. Estimation of the macromolecular proton fraction and bound pool T2 in multiple sclerosis. Mult. Scler. 10, 607–613. https://doi.org/10.1191/1352458504ms1105oa.

Dehmeshki, J., Chard, D.T., Leary, S.M., Watt, H.C., Silver, N.C., Tofts, P.S., Thompson, A.J., Miller, D.H., 2003. The normal appearing grey matter in primary progressive multiple sclerosis. J. Neurol. 250, 67–74. https://doi.org/10.1007/s00415-003-0955-x.

Deoni, S.C.L., Rutt, B.K., Arun, T., Pierpaoli, C., Jones, D.K., 2008. Gleaning multicomponent T1 and T2 information from steady-state imaging data. Magn. Reson. Med. 60, 1372–1387. https://doi.org/10.1002/mrm.21704.

Ernst, A., Noblet, V., Gounot, D., Blanc, F., de Seze, J., Manning, L., 2015. Neural correlates of episodic future thinking impairment in multiple sclerosis patients. J. Clin. Exp. Neuropsychol. 37, 1107–1123. https://doi.org/10.1080/13803395.2015.1080228.

Filippi, M., Rocca, M.A., Barkhof, F., Brück, W., Chen, J.T., Comi, G., DeLuca, G., De Stefano, N., Erickson, B.J., Evangelou, N., Fazekas, F., Geurts, J.J.G., Lucchinetti, C., Miller, D.H., Pelletier, D., Popescu, B.F.G., Lassmann, H., 2012. Association between pathological and MRI findings in multiple sclerosis. Lancet Neurol. 11, 349–360. https://doi.org/10.1016/S1474-4422(12)70003-0.

Friston, K.J., Holmes, A.P., Poline, J.B., Grasby, P.J., Williams, S.C., Frackowiak, R.S., Turner, R., 1995. Analysis of fMRI time-series revisited. Neuroimage 2, 45–53. https://doi.org/10.1006/nimg.1995.1007.

Ge, Y., Grossman, R.I., Udupa, J.K., Babb, J.S., Kolson, D.L., McGowan, J.C., 2001. Magnetization transfer ratio histogram analysis of gray matter in relapsing-remitting multiple sclerosis. AJNR Am. J. Neuroradiol. 22, 470–475.

Geisseler, O., Pflugshaupt, T., Bezzola, L., Reuter, K., Weller, D., Schuknecht, B., Brugger, P., Linnebank, M., 2016. Cortical thinning in the anterior cingulate cortex predicts multiple sclerosis patients’ fluency performance in a lateralised manner. NeuroImage

Clin. 10, 89–95. https://doi.org/10.1016/j.nicl.2015.11.008.
Gracien, R., Jurcoane, A., Wagner, M., Reitz, S.C., 2016. The relationship between gray matter quantitative MRI and disability in secondary progressive multiple sclerosis 1, 1–14. 10.1371/journal.pone.0161036.
Griffin, C.M., Chard, D.T., Ciccarelli, O., Kapoor, R., Barker, G.J., Thompson, A.J., Miller, D.H., 2001. Diffusion tensor imaging in early relapsing-remitting multiple sclerosis. Mult. Scler. J. 7, 290–297. https://doi.org/10.1177/135245850100700504.
Hayton, T., Furby, J., Smith, K.J., Altmann, D.R., Brenner, R., Chataway, J., Hughes, R.A.C., Hunter, K., Tozer, D.J., Miller, D.H., Kapoor, R., 2009. Grey matter magnetization transfer ratio independently correlates with neurological deficit in secondary progressive multiple sclerosis. J. Neurol. 256, 427–435. https://doi.org/10.1007/s00415-009-0110-4.
Keser, Z., Hasan, K.M., Mwangi, B., Gabr, R.E., Steinberg, J.L., Wilken, J., Wolinsky, J.S., Nelson, F.M., 2017. Limbic pathway correlates of cognitive impairment in multiple sclerosis. J. Neuroimaging 27, 37–42. https://doi.org/10.1111/jon.12381.
Keser, Z., Hasan, K.M., Mwangi, B., Younes, K., Khayat-Khoei, M., Kamali, A., Lincoln, J.A., Nelson, F.M., 2018. Quantitative limbic system mapping of main cognitive domains in multiple sclerosis. Front. Neurol. 9, 132. https://doi.org/10.3389/fneur.2018.00132.
Khaleeli, Z., Cercignani, M., Audoin, B., Ciccarelli, O., Miller, D.H., Thompson, A.J., 2007. Localized grey matter damage in early primary progressive multiple sclerosis contributes to disability. Neuroimage 37, 253–261. https://doi.org/10.1016/j.neuroimage.2007.04.056.
Khalil, M., Langkammer, C., Pichler, A., Pinter, D., Gattringer, T., Bachmaier, G., Ropele, S., Fuchs, S., Enzinger, C., Fazekas, F., 2015. Dynamics of brain iron levels in multiple sclerosis. Neurology 84, 1–8.
Kolbe, S.C., Kilpatrick, T.J., Mitchell, P.J., White, O., Egan, G.F., Fielding, J., 2014. Inhibitory saccadic dysfunction is associated with cerebellar injury in multiple sclerosis. Hum. Brain Mapp. 35, 2310–2319. https://doi.org/10.1002/hbm.22329.
Kutzelnigg, A., Lucchinetti, C.F., Stadelmann, C., Brück, W., Rauschka, H., Bergmann, M., Schmidbauer, M., Parisi, J.E., Lassmann, H., 2005. Cortical demyelination and diffuse white matter injury in multiple sclerosis. Brain 128, 2705–2712. https://doi.org/10.1093/brain/awh641.
Lansley, J., Mataix-Cols, D., Grau, M., Radua, J., Sastre-Garriga, J., 2013. Localized grey matter atrophy in multiple sclerosis: a meta-analysis of voxel-based morphometry studies and associations with functional disability. Neurosci. Biobehav. Rev. 37, 819–830. https://doi.org/10.1016/j.neubiorev.2013.03.006.
Laule, C., Leung, E., Li, D.K., Traboulsee, A.L., Paty, D.W., MacKay, A.L., Moore, G.R., 2006. Myelin water imaging in multiple sclerosis: quantitative correlations with histopathology. Mult. Scler. J. 12, 747–753. https://doi.org/10.1177/1352458506070928.
Llufriu, S., Martinez-Heras, E., Fortea, J., Blanco, Y., Berenguer, J., Gabilondo, I., Ibarretxe-Bilbao, N., Falcon, C., Sepulveda, M., Sola-Valls, N., Bargallo, N., Graus, F., Villoslada, P., Saiz, A., 2014. Cognitive functions in multiple sclerosis: impact of gray matter integrity. Mult. Scler. J. 20, 424–432. https://doi.org/10.1177/1352458513503722.
Louapre, C., Govindarajan, S.T., Giannì, C., Cohen-Adad, J., Gregory, M.D., Nielsen, A.S., Madigan, N., Sloane, J.A., Kinkel, R.P., Mainero, C., 2016a. Is the relationship between cortical and white matter pathologic changes in multiple sclerosis spatially specific? A multimodal 7-T and 3-T MR imaging study with surface and tract-based analysis. Radiology 278, 524–535. https://doi.org/10.1148/radiol.2015150486.
Louapre, C., Govindarajan, S.T., Giannì, C., Madigan, N., Nielsen, A.S., Sloane, J.A., Kinkel, R.P., Mainero, C., 2016b. The association between intra- and juxta-cortical pathology and cognitive impairment in multiple sclerosis by quantitative T2* mapping at 7 T MRI. NeuroImage Clin. 12, 879–886. https://doi.org/10.1016/j.nicl.2016.11.001.
Lund, H., Jønsson, A., Andresen, J., Rostrup, E., Paulson, O.B., Sørensen, P.S., 2012. Cognitive deficits in multiple sclerosis: correlations with T2 changes in normal appearing brain tissue. Acta Neurol. Scand. 125, 338–344. https://doi.org/10.1111/j.1600-0404.2011.01574.x.
Mainero, C., Louapre, C., Govindarajan, S.T., Giannì, C., Nielsen, A.S., Cohen-Adad, J., Sloane, J., Kinkel, R.P., 2015. A gradient in cortical pathology in multiple sclerosis by in vivo quantitative 7T imaging. Brain 138, 932–945. https://doi.org/10.1093/brain/awv011.
Marques, J.P., Kober, T., Krueger, G., van der Zwaag, W., Van de Moortele, P.-F., Gruetter, R., 2010. MP2RAGE, a self bias-field corrected sequence for improved segmentation and T1-mapping at high field. Neuroimage 49, 1271–1281. https://doi.org/10.1016/j.neuroimage.2009.10.002.
McDonald, W.I., Compston, A., Edan, G., Goodkin, D., Hartung, H.P., Lublin, F.D., McFarland, H.F., Paty, D.W., Polman, C.H., Reingold, S.C., Sandberg-Wollheim, M., Sibley, W., Thompson, A., van den Noort, S., Weinshenker, B.Y., Wolinsky, J.S., 2001. Recommended diagnostic criteria for multiple sclerosis: guidelines from the International Panel on the diagnosis of multiple sclerosis. Ann. Neurol. 50, 121–127.
Megna, R., Alfano, B., Lanzillo, R., Costabile, T., Comerci, M., Vacca, G., Carotenuto, A., Moccia, M., Servillo, G., Prinster, A., Brescia Morra, V., Quarantelli, M., 2019. Brain tissue volumes and relaxation rates in multiple sclerosis: implications for cognitive impairment. J. Neurol. 266, 361–368. https://doi.org/10.1007/s00415-018-9139-6.
Nakamura, K., Chen, J.T., Ontaneda, D., Fox, R.J., Trapp, B.D., 2017. T1-/T2-weighted ratio differs in demyelinated cortex in multiple sclerosis. Ann. Neurol. 82, 635–639. https://doi.org/10.1002/ana.25019.
Neema, M., Stankiewicz, J., Arora, A., Dandamudi, V.S.R., Batt, C.E., Guss, Z.D., Al-Sabbagh, A., Bakshi, R., 2007. T1- and T2-based MRI measures of diffuse gray matter and white matter damage in patients with multiple sclerosis. J. Neuroimaging 17, 16–21. https://doi.org/10.1111/j.1552-6569.2007.00131.x.
Nocentini, U., Bozzali, M., Spanò, B., Cercignani, M., Serra, L., Basile, B., Mannu, R., Caltagirone, C., De Luca, J., 2014. Exploration of the relationships between regional grey matter atrophy and cognition in multiple sclerosis. Brain Imaging Behav. 8, 378–386. https://doi.org/10.1007/s11682-012-9170-7.
Palma, G., Tedeschi, E., Borrelli, P., Cocozza, S., Russo, C., Liu, S., Ye, Y., Comerci, M., Alfano, B., Salvatore, M., Haacke, E.M., Mancini, M., 2015. A novel multiparametric approach to 3 D quantitative MRI of the brain. PLoS One 10, e0134963. https://doi.org/10.1371/journal.pone.0134963.
Popescu, V., Schoonheim, M.M., Versteeg, A., Chaturvedi, N., Jonker, M., Xavier de Menezes, R., Gallindo Garre, F., Uitdehaag, B.M.J., Barkhof, F., Vrenken, H., 2016. Grey matter atrophy in multiple sclerosis: clinical interpretation depends on choice of analysis method. PLoS One 11, e0143942. https://doi.org/10.1371/journal.pone.0143942.
Pota, M., Esposito, M., Megna, R., De Pietro, G., Quarantelli, M., Brescia Morra, V., Alfano, B., 2019. Multivariate fuzzy analysis of brain tissue volumes and relaxation rates for supporting the diagnosis of relapsing-remitting multiple sclerosis. Biomed. Signal Process. Control 53. https://doi.org/10.1016/j.bspc.2019.101591.
Preziosa, P., Rocca, M.A., Pagani, E., Stromillo, M.L., Enzinger, C., Gallo, A., Hulst, H.E., Atzori, M., Pareto, D., Riccitelli, G.C., Copetti, M., De Stefano, N., Fazekas, F., Bisecco, A., Barkhof, F., Yousry, T.A., Arévalo, M.J., Filippi, M., 2016. Structural MRI correlates of cognitive impairment in patients with multiple sclerosis: a Multicenter Study. Hum. Brain Mapp. 37, 1627–1644. https://doi.org/10.1002/hbm.23125.
Prinster, A., Quarantelli, M., Lanzillo, R., Orefice, G., Vacca, G., Carotenuto, B., Alfano, B., Brunetti, A., Brescia Morra, V., Salvatore, M., 2010. A voxel-based morphometry study of disease severity correlates in relapsing- remitting multiple sclerosis. Mult. Scler. 16, 45–54. https://doi.org/10.1177/1352458509351896.
Prinster, A., Quarantelli, M., Orefice, G., Lanzillo, R., Brunetti, A., Mollica, C., Salvatore, E., Morra, V.B., Coppola, G., Vacca, G., Alfano, B., Salvatore, M., 2006. Grey matter loss in relapsing-remitting multiple sclerosis: a voxel-based morphometry study. Neuroimage 29, 859–867. https://doi.org/10.1016/j.neuroimage.2005.08.034.
Quinn, M.P., Gati, J.S., Klassen, M.L., Lee, D.H., Kremenchutzky, M., Menon, R.S., 2014. Increased deep gray matter iron is present in clinically isolated syndromes. Mult. Scler. Relat. Disord. 3, 194–202. https://doi.org/10.1016/j.msard.2013.06.017.
Ramio-Torrenta, L., Sastre-Garriga, J., Ingle, G.T., Davies, G.R., Ameen, V., Miller, D.H., Thompson, A.J., 2006. Abnormalities in normal appearing tissues in early primary progressive multiple sclerosis and their relation to disability: a tissue specific magnetisation transfer study. J. Neurol. Neurosurg. Psychiatry 77, 40–45. https://doi.org/10.1136/jnnp.2004.052316.
Ranjeva, J.-P., Audoin, B., Duong, A., Van, M., Confort-Gouny, S., Malikova, I., Viout, P., Soulier, E., Pelletier, J., Cozzone, P.J., 2006. Structural and functional surrogates of cognitive impairment at the very early stage of multiple sclerosis. J. Neurol. Sci. 245, 161–167. https://doi.org/10.1016/j.jns.2005.09.019.
Ranjeva, J.-P., Audoin, B., Duong, A., Van, M., Duong, M.V.A., Ibarrola, D., Confort-Gouny, S., Malikova, I., Soulier, E., Viout, P., Ali-Chérif, A., Pelletier, J., Cozzone, P., 2005. Local tissue damage assessed with statistical mapping analysis of brain magnetization transfer ratio: relationship with functional status of patients in the earliest stage of multiple sclerosis. AJNR Am. J. Neuroradiol. 26, 119–127.
Rao, S.M., 1991 . A manual for the brief, Repeatable Battery of Neuropsychological Tests in Multiple Sclerosis National Multiple Sclerosis Society.
Riccitelli, G., Rocca, M.A., Pagani, E., Rodegher, M.E., Rossi, P., Falini, A., Comi, G., Filippi, M., 2011. Cognitive impairment in multiple sclerosis is associated to different patterns of gray matter atrophy according to clinical phenotype. Hum. Brain Mapp. 32, 1535–1543. https://doi.org/10.1002/hbm.21125.
Rovaris, M., Judica, E., Sastre-Garriga, J., Rovira, A., Pia Sormani, M., Benedetti, B., Korteweg, T., De Stefano, N., Khaleeli, Z., Montalban, X., Barkhof, F., Miller, D.H., Polman, C., Thompson, A.J., Filippi, M., 2008. Large-scale, multicentre, quantitative MRI study of brain and cord damage in primary progressive multiple sclerosis. Mult. Scler. J. 14, 455–464. https://doi.org/10.1177/1352458507085129.
Rudko, D.A., Solovey, I., Gati, J.S., Kremenchutzky, M., Menon, R.S., Rsna, Q., 2014. Multiple sclerosis: improved identification of disease-relevant changes in gray and white matter by using susceptibility-based MR imaging. Radiology 272, 851–864. https://doi.org/10.1148/radiol.14132475.
Samson, R.S., Cardoso, M.J., Muhlert, N., Sethi, V., Wheeler-Kingshott, C.A., Ron, M., Ourselin, S., Miller, D.H., Chard, D.T., 2014. Investigation of outer cortical magnetisation transfer ratio abnormalities in multiple sclerosis clinical subgroups. Mult. Scler. J. 20, 1322–1330. https://doi.org/10.1177/1352458514522537.
Samson, R.S., Muhlert, N., Sethi, V., Wheeler-Kingshott, C.A.M., Ron, M.A., Miller, D.H., Chard, D., 2013. Sulcal and gyral crown cortical grey matter involvement in multiple sclerosis: a magnetisation transfer ratio study. Mult. Scler. Relat. Disord. 2, 204–212. https://doi.org/10.1016/j.msard.2013.01.001.
Sbardella, E., Petsas, N., Tona, F., Prosperini, L., Raz, E., Pace, G., Pozzilli, C., Pantano, P., 2013. Assessing the correlation between grey and white matter damage with motor and cognitive impairment in multiple sclerosis patients. PLoS One 8, e63250. https://doi.org/10.1371/journal.pone.0063250.
Schmierer, K., Parkes, H.G., So, P.-W., An, S.F., Brandner, S., Ordidge, R.J., Yousry, T.A., Miller, D.H., 2010. High field (9.4 Tesla) magnetic resonance imaging of cortical grey matter lesions in multiple sclerosis. Brain 133, 858–867. https://doi.org/10.1093/brain/awp335.
Seewann, A., Vrenken, H., Kooi, E.-J., van der Valk, P., Knol, D.L., Polman, C.H., Pouwels, P.J.W., Barkhof, F., Geurts, J.J.G., 2011. Imaging the tip of the iceberg: visualization of cortical lesions in multiple sclerosis. Mult. Scler. 17, 1202–1210. https://doi.org/10.1177/1352458511406575.
Senda, J., Watanabe, H., Tsuboi, T., Hara, K., Watanabe, H., Nakamura, R., Ito, M., Atsuta, N., Tanaka, F., Naganawa, S., Sobue, G., 2012. MRI mean diffusivity detects widespread brain degeneration in multiple sclerosis. J. Neurol. Sci. 319, 105–110. https://doi.org/10.1016/j.jns.2012.04.019.
Tzourio-Mazoyer, N., Landeau, B., Papathanassiou, D., Crivello, F., Etard, O., Delcroix, N., Mazoyer, B., Joliot, M., 2002. Automated anatomical labeling of activations in SPM

using a macroscopic anatomical parcellation of the MNI MRI single-subject brain. Neuroimage 15, 273–289. https://doi.org/10.1006/nimg.2001.0978.

van de Pavert, S.H.P., Muhlert, N., Sethi, V., Wheeler-Kingshott, C.A.M., Ridgway, G.R., Geurts, J.J.G., Ron, M., Yousry, T.A., Thompson, A.J., Miller, D.H., Chard, D.T., Ciccarelli, O., 2016. DIR-visible grey matter lesions and atrophy in multiple sclerosis: partners in crime? J. Neurol. Neurosurg. Psychiatry 87, 461–467. https://doi.org/10.1136/jnnp-2014-310142.

Vrenken, H., Pouwels, P.J.W., Ropele, S., Knol, D.L., Geurts, J.J.G., Polman, C.H., Barkhof, F., Castelijns, J.A., 2007. Magnetization transfer ratio measurement in multiple sclerosis normal-appearing brain tissue: limited differences with controls but relationships with clinical and MR measures of disease. Mult. Scler. J. 13, 708–716. https://doi.org/10.1177/1352458506075521.

Wen, J., Yablonskiy, D.A., Luo, J., Lancia, S., Hildebolt, C., Cross, A.H., 2015. Detection and quantification of regional cortical gray matter damage in multiple sclerosis utilizing gradient echo MRI. NeuroImage Clin. 9, 164–175. https://doi.org/10.1016/j.nicl.2015.08.003.

Wen, J., Yablonskiy, D.A., Salter, A., Cross, A.H., 2017. Limbic system damage in MS: MRI assessment and correlations with clinical testing. PLoS One 12, e0187915. https://doi.org/10.1371/journal.pone.0187915.

Yarnykh, V.L., Bowen, J.D., Samsonov, A., Repovic, P., Mayadev, A., Qian, P., Gangadharan, B., Keogh, B.P., Maravilla, K.R., Jung Henson, L.K., 2015. Fast whole-brain three-dimensional macromolecular proton fraction mapping in multiple sclerosis. Radiology 274, 210–220. https://doi.org/10.1148/radiol.14140528.

Yu, C.S., Lin, F.C., Liu, Y., Duan, Y., Lei, H., Li, K.C., 2008. Histogram analysis of diffusion measures in clinically isolated syndromes and relapsing-remitting multiple sclerosis. Eur. J. Radiol. 68, 328–334. https://doi.org/10.1016/j.ejrad.2007.08.036.

Zhang, X., Zhang, F., Huang, D., Wu, L., Ma, L., Liu, H., Zhao, Y., Yu, S., Shi, J., 2016. Contribution of gray and white matter abnormalities to cognitive impairment in multiple sclerosis. Int. J. Mol. Sci. 18, 46. https://doi.org/10.3390/ijms18010046.